OCEAN ACOUSTIC WAVEGUIDE INVARIANT PARAMETER ESTIMATION USING TONAL NOISE SOURCES

Andrew Harms, Jonathan L. Odom, and Jeffrey L. Krolik

Duke University, Durham, NC 27708
andrew.harms@duke.edu, jonathan.l.odom@ieee.org, jlk@duke.edu

ABSTRACT

The abundance of shipping noise sources in ocean littoral zones provides a great opportunity to estimate ocean environmental parameters. The waveguide invariant parameter β, defined as the ratio of inverse group and phase velocities between modes, has been used in a variety of applications including ranging of passive sources. Previous work utilizing the waveguide invariant in passive sonar has relied on processing the time-frequency intensity striations of broadband sources. In this paper, the reception of strong tonal components from transiting commercial ships of known location (e.g., from AIS data) are used for estimating β over the source-receiver path. A maximum likelihood estimate of β is derived by relating the fading characteristics of different tonal components over range. The method is verified on simulated data using a Pekeris waveguide model.

Index Terms— Maximum Likelihood, Waveguide Invariant

1. INTRODUCTION

The waveguide invariant parameter encapsulates the dispersive propagation properties of an environment with a scalar parameter. The parameter is approximately constant over large areas in many environments, including shallow water that is often dominated by anthropogenic noise at lower frequencies (less than several kHz) [1]. While previous methods have focused on exploiting broadband data to estimate the waveguide invariant parameter or source range, this paper considers tonal sources. Merchant ships in littoral zones create acoustic noise with strong tonal components that can be exploited to both separate sources in frequency and estimate propagation parameters [2].

Traditionally, waveguide invariance has been analyzed in terms of the patterns that emerge in intensity plots of the spectrogram of acoustic data. The interference patterns from the superposition of direct-path and multi-path waves within the waveguide form lines of constant intensity in range and frequency, commonly called striation patterns. These striations patterns for broadband sources are well documented and can be interpreted using various waveguide models [3]. Using normal mode theory, the striations are a result of a nearly linear relationship between group and phase slowness for neighboring modes. The parameter of interest is called the waveguide invariant parameter and denoted by β. It is defined as the ratio of group to phase slowness, which is approximately constant across modes and space. In terms of range r and frequency ω, β is defined through lines of constant intensity I determined by

$$\frac{\partial I}{\partial \omega}\delta\omega + \frac{\partial I}{\partial r}\delta r = 0. \quad (1)$$

The striation patterns occur at ranges as close as several water column depths away, which is particularly important in shallow water [4]. Previous work has shown that source range can be estimated with very little environmental knowledge since only a single scalar parameter must be known instead of entire sound speed profiles [5]. Recent work has considered broadband and tonal data to estimate range using cross-correlations in terms of the closest point of arrival [6], beamforming [7], and active sonar [8]. However, passive estimation of β has primarily relied on image processing techniques such as Hough transforms or integrating along estimated striation lines [9] or wavenumber integration techniques [10].

Cargo ships generate strong narrowband components that, in principle, can be separated based on their frequency content [2]. To leverage such opportunistic sources, this paper considers tonal sources, where multiple narrowband frequencies are simultaneously emitted by a single source that is moving away from the receiver. The relative range and range rate between the source and receiver are assumed known at constant depth. Waveguide invariant theory and the resulting model are summarized in Section 2. The proposed waveguide invariant parameter estimate is derived in Section 3, and simulation of a Pekeris waveguide is used to demonstrate the feasibility of estimating the waveguide invariant using tonal sources in a noisy environment in Section 4.

2. THE WAVEGUIDE INVARIANT

The waveguide invariant phenomena was first investigated in [3] and further analyzed in [4]. We briefly summarize the phenomena in the context of a normal mode propagation model after first setting up the tonal source signal model.

2.1. Source Signal Model

A source at depth z_s generates an acoustic pressure signal $s(t)$ of constant (frequency-dependent) amplitude $a(\omega)$ with an unknown, uniformly distributed phase $\phi(\omega) \sim \mathcal{U}(-\pi, \pi]$ that is constant over time:

$$s(t) = \sum_{\omega \in \Omega} a(\omega) \mathrm{e}^{j(\omega t + \phi(\omega))}. \tag{2}$$

The frequency index set Ω is continuous in the case of broadband sources, but in this paper we consider a finite discrete set to model a tonal source.

2.2. Normal Mode Propagation Model

The normal-mode acoustic pressure field

$$p(r,t) = \sum_{\omega} p(r,\omega,t) \tag{3}$$

can be broken into pieces that are a function of range (from source to receiver), frequency, and time:

$$p(r,\omega,t) = \frac{a(\omega)}{\sqrt{r}} \sum_{m=1}^{M} \frac{A_m(z)}{\sqrt{k_m(\omega)}} \mathrm{e}^{j(k_m(\omega) r - \omega t - \phi(\omega))} \tag{4}$$

where $k_m(\omega)$ is the horizontal wavenumber (mode eigenvalue) and $A_m(z) = \Psi_m(z)\Psi_m(z_s)$ is the mode eigenfunction (at the source and receiver) for the m^{th} mode. In the remainder of this paper, we assume that the source and receiver are at a constant depth so that $A_m(z)$ are constant.

The intensity of the received acoustic pressure field is

$$\begin{aligned} I(r,\omega) &= p^*(r,\omega,t) p(r,\omega,t) \\ &= \frac{a(\omega)^2}{r} \sum_{m,n=1}^{M} \frac{A_m(z) A_n(z)}{\sqrt{k_m(\omega) k_n(\omega)}} \mathrm{e}^{j \Delta k_{mn}(\omega) r} \end{aligned} \tag{5}$$

where $\Delta k_{mn}(\omega) = (k_m(\omega) - k_n(\omega))$ is the wavenumber difference. Notice the intensity does not depend on time.

2.3. Intensity Fading Patterns

The waveguide invariant describes the interference pattern of the received *intensity* of the sound pressure field. Loci of constant intensity occur when the total derivative vanishes, i.e., $dI = 0$. Considering frequency ω and range r, we have

$$dI(r,\omega) = \frac{\partial I(r,\omega)}{\partial \omega} \delta\omega + \frac{\partial I(r,\omega)}{\partial r} \delta r = 0. \tag{6}$$

Substituting (5) into (6) and considering two modes, we get [4, Equation (12)]

$$\frac{\delta r}{\delta \omega} = -\frac{r}{\omega} \frac{\partial \Delta k_{mn}(\omega)/\partial \omega}{\Delta k_{mn}(\omega)/\omega} = \frac{r}{\omega} \frac{1}{\beta}. \tag{7}$$

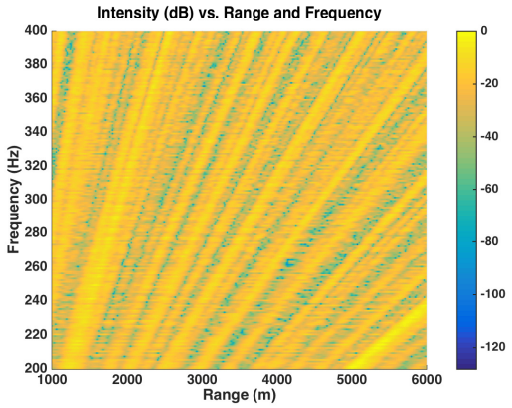

Fig. 1: Received intensity in dB as a function of frequency and range from a broadband source. The striations, or lines of constant intensity, follow (11) with $\beta \approx 1$.

The quantity

$$\frac{1}{\beta} = -\frac{\partial \Delta k_{mn}(\omega)/\partial \omega}{\Delta k_{mn}(\omega)/\omega} \tag{8}$$

is the ratio of inverse group velocity to inverse phase velocity and is approximately invariant for a group of propagating modes, i.e., (8) is approximately constant for all m, n [4]. The relation (7) therefore holds for each term of the sum in (5) and defines the conditions for the loci of constant intensity, $dI = 0$. Rearranging (7) yields $(\delta r/r)\beta = (\delta\omega/\omega)$, and we integrate both sides to get

$$\omega = \omega_0 \left(\frac{r}{r_0} \right)^{\beta} \tag{9}$$

where ω_0 and r_0 are a reference frequency and range. For sources consisting of tonal signals with known, or well-estimated, frequencies, an equivalent form is more relevant:

$$r = r_0 \left(\frac{\omega}{\omega_0} \right)^{1/\beta}. \tag{10}$$

The intensity at an arbitrary range and frequency can be related to the intensity at a reference range and frequency:

$$I(r,\omega) = I\left(r_0 \left(\frac{\omega}{\omega_0} \right)^{1/\beta}, \omega_0 \right). \tag{11}$$

Relation (11) defines the loci of constant intensity, which are lines for $\beta = 1$. Fig. 1 shows an example intensity plot as a function of frequency and range for a broadband noise source in a Pekeris waveguide, for which $\beta \approx 1$ [1]. The lines of constant intensity seen in the plot follow (11). Fig. 2 shows the intensity for a source emitting three tones.

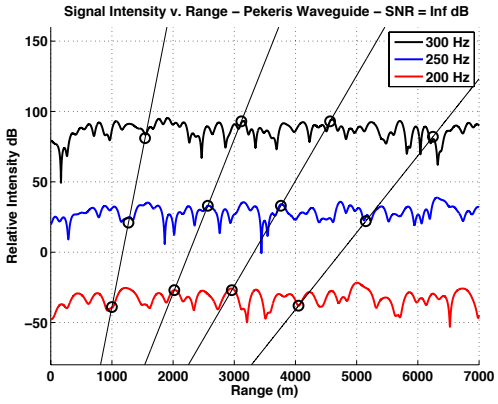

Fig. 2: Received intensity as a function of range from a source generating three tones in a Pekeris waveguide. The three intensities are placed on the same relative scale and each is offset by 50 dB. Several lines are drawn between the curves to show the points of equal intensity that satisfy (11).

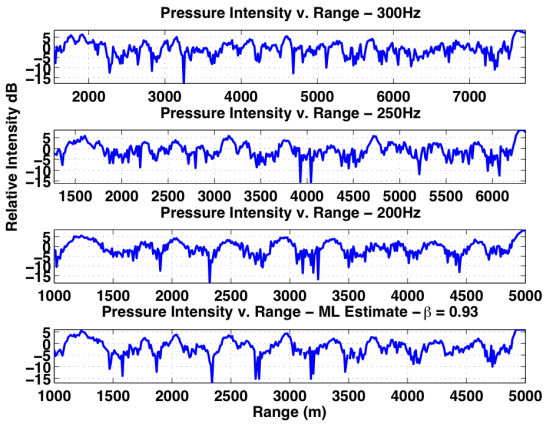

Fig. 3: ML estimate of the intensity profile for hypothesized $\beta = 0.93$. The first three plots show the received intensity profile at three frequencies with range scaling corresponding to the hypothesized β. The intensity is generated using a Pekeris waveguide model and has noise added so that the SNR is 10 dB. Visually, the matching is pretty good because the peaks and valleys in each plot generally match.

3. ESTIMATING THE WAVEGUIDE INVARIANT

In this section, we propose an estimator for the waveguide invariant parameter β using intensity data from a discrete set of known frequencies. The key is the appropriate scaling of the range axis at each frequency in the intensity data according to (11). Because the frequencies are known, the scaling is entirely dependent on β. The estimator uses a joint maximum likelihood (ML) and (empirical) minimum mean-squared error (MMSE) criterion to find the *best* value of β that explains the intensity data. We first introduce the noise model before describing the estimator.

3.1. Noise Model for Intensity Data

The noise model introduces complex circularly symmetric Gaussian noise into the pressure field (3). Let $n(r,t) \sim \mathcal{CN}(0,\sigma^2)$ be the noise added to the pressure field (3):

$$p_{\text{noisy}}(r,t) = p(r,t) + n(r,t). \tag{12}$$

The noisy intensity is

$$\begin{aligned} I_{\text{noisy}}(r,\omega) &= p^*_{\text{noisy}}(r,t)p_{\text{noisy}}(r,t) \\ &= |\sqrt{I(r,\omega)} + n(r,\omega)|^2 \end{aligned} \tag{13}$$

where $I(r,\omega)$ is the intensity without noise and $n(r,\omega) \sim \mathcal{CN}(0,\sigma^2)$. The noisy intensity is a scaled non-central chi-squared distributed random variable with non-centrality parameter $\lambda = I(r,\omega)/\sigma^2$. To be more precise, let $Y = \sigma^2 I_{\text{noisy}}(r,\omega)$ with distribution

$$f_Y(y; I(r,\omega), \sigma^2) = \frac{1}{2} \mathrm{e}^{\frac{-(y+I(r,\omega))}{2\sigma^2}} I_0\left(\frac{\sqrt{yI(r,\omega)}}{\sigma^2}\right) \tag{14}$$

where $I_0(\cdot)$ is a modified Bessel function of the first kind.

3.2. ML Estimate of Intensity

The estimator consists of two steps. The first step is an ML estimate of the signal intensity, based on the correct hypothesized value of β. For the correct hypothesized β, the noiseless intensity (at appropriately scaled ranges given by (11)) is constant. Fig. 2 provides a visualization of the (noiseless) intensity at three frequencies, each separated by 50 Hz, for a Pekeris waveguide model. The lines connecting the intensity profiles are for $\beta = 1$ in (11), which is close to the true value for a Pekeris waveguide. The peaks or valleys in the intensity match pretty well along these lines at each frequency. To make this more precise, consider a set of F frequencies denoted ω_i for $i = 1,\ldots,F$ and a set of N range samples referenced to the intensity profile at ω_1 and denoted $r_1(n)$ for $n = 1,\ldots,N$. The range values at every other frequency with the same (noiseless) intensity are given by (11), i.e., $r_i(n) = r_1(n)\left(\omega_i/\omega_1\right)^{1/\beta}$ and

$$I\left(r_i(n),\omega_i\right) = I\left(r_1(n)\left(\frac{\omega_i}{\omega_1}\right)^{1/\beta}, \omega_1\right). \tag{15}$$

Since the received intensity data is noisy, the correct value of β in (15) means that the random variables across frequency (i.e., across i) are independent identically distributed (IID). Denote the noiseless intensity, appropriately scaled according to (15), as $I(n;\beta) = I(r_i(n),\omega_i)\ \forall i$. The likelihood function given noisy data $y_i(n) = I_{\text{noisy}}(r_i(n),\omega_i)$ is

$$\ell\left(I(n;\beta)\middle|\{y_i(n)\}\right) = \prod_{i=1}^{F} f_Y\left(y_i(n); I(n;\beta), \sigma^2\right). \tag{16}$$

The ML estimate for a hypothesized value of β is thus

$$\hat{I}(n;\beta) = \arg\max_{I(n;\beta)} \ell\left(I(n;\beta)|\left\{y_i(n)\right\}\right). \qquad (17)$$

Fig. 3 shows an example of the ML estimate using received noisy intensity data at three frequencies each at 10 dB signal-to-noise ratio (SNR). The hypothesized $\beta = 0.93$ is close to the true value, so the ML estimate visually matches each received intensity pretty well. The mean squared error of the three intensity curves to the ML estimate is approximately -2 dB.

3.3. MMSE-ML Estimate of β

The ML intensity (17) is a function of n and β. Each hypothesized value of β results in a different ML estimate of the intensity as a function of n (reference ranges) due to the different scalings of the range axis, given by (15). The second step of the estimator calculates the mean-square error (MSE) between the ML intensity $\hat{I}(n;\beta)$ and the received intensity data $y_i(n)$ as a function of β, i.e.,

$$\text{MSE}(\beta) = \frac{1}{FN}\sum_{n=1}^{N}\sum_{i=1}^{F}\left(\hat{I}(n;\beta) - y_i(n)\right)^2. \qquad (18)$$

The MMSE estimate minimizes this empirical error:

$$\hat{\beta} = \arg\min_{\beta} \text{MSE}(\beta). \qquad (19)$$

4. NUMERICAL RESULTS AND DISCUSSION

Monte Carlo simulations over noise realizations were performed to test the ML-MMSE estimator of β. Fig. 4 shows the result of 5 simulations using three frequencies. The noiseless intensites were generated using the normal mode model from Section 2.2 for a Pekeris waveguide with a single source at a depth of 54 m and receiver at a depth of 150 m. For this scenario, it is known that $\beta \approx 1$ [4]. Table 1 summarizes the results from 1000 Monte Carlo trials.

Table 1: Summary of Monte Carlo simulation results using three frequencies (200 Hz, 250 Hz, and 300 Hz) and varying SNR of the intensity data. The SNR indicated is per tone.

SNR (dB)	Mean $\hat{\beta}$	Std. Dev. $\hat{\beta}$
0	0.917	0.194
10	0.934	0.007
20	0.933	0.004
30	0.932	0.002

5. REFERENCES

[1] F. B. Jensen, W. A. Kuperman, M. B. Porter, and H. Schmidt, *Computational Ocean Acoustics*, Springer, 2011.

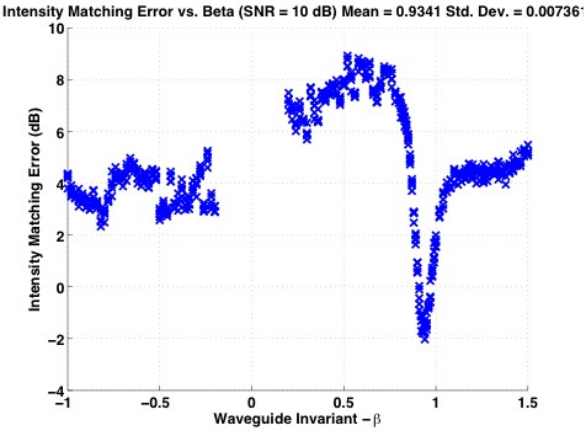

Fig. 4: Results from 5 simulations of the MSE calculation (18) using three frequencies (200 Hz, 250 Hz, and 300 Hz).

[2] P.T. Arveson and D.J. Vendittis, "Radiated noise characteristics of a modern cargo ship," *J. Acoust. Soc. Am.*, vol. 107, no. 1, pp. 118–129, Jan 2000.

[3] S.D. Chuprov, "Interference structure of a sound field in a layered ocean," *Ocean Acoustics, Current State*, 1982.

[4] G. L. D'Spain and W. A. Kuperman, "Application of waveguide invariants to analysis of spectrograms from shallow water environments that vary in range and azimuth," *J. Acoust. Soc. Am.*, vol. 106, no. 5, pp. 2454–2468, Nov 1999.

[5] A.M. Thode, "Source ranging with minimal environmental information using a virtual receiver and waveguide invariant theory," *J. Acoust. Soc. Am.*, vol. 108, no. 4, pp. 1582–94, Oct 2000.

[6] S.T. Rakotonarivo and W.A. Kuperman, "Model-independent range localization of a moving source in shallow water," *J. Acoust. Soc. Am.*, vol. 132, no. 4, pp. 2218–23, 2012.

[7] Hailiang Tao and Jeffrey L. Krolik, "Waveguide invariant focusing for broadband beamforming in an oceanic waveguide," *J. Acoust. Soc. Am.*, vol. 123, pp. 1338–46, 2008.

[8] J.E. Quijano, L.M. Zurk, and D. Rouseff, "Demonstration of the invariance principle for active sonar," *J. Acoust. Soc. Am.*, vol. 123, pp. 1329–37, 2008.

[9] K.L. Cockrell and H. Schmidt, "Robust passive range estimation using the waveguide invariant," *J. Acoust. Soc. Am.*, vol. 127, no. 5, pp. 2780–89, 2010.

[10] K. L. Cockrell and H. Schmidt, "A relationship between the waveguide invariant and wavenumber integration," *J. Acoust. Soc. Am. Express Letters*, vol. 128, no. 1, pp. 63–68, 2010.